PHILOSOPHICAL TRANSACTIONS OF THE ROYAL SOCIETY A MATHEMATICAL, PHYSICAL & ENGINEERING SCIENCES

Hysteretic effects of dry friction: modelling and experimental studies

Jerzy Wojewoda, Andrzej Stefanski, Marian Wiercigroch and Tomasz Kapitaniak

Phil. Trans. R. Soc. A 2008 **366**, 747-765
doi: 10.1098/rsta.2007.2125

PHILOSOPHICAL TRANSACTIONS OF THE ROYAL SOCIETY A

Phil. Trans. R. Soc. A (2008) **366**, 747–765
doi:10.1098/rsta.2007.2125
Published online 18 October 2007

Hysteretic effects of dry friction: modelling and experimental studies

By Jerzy Wojewoda[1,*], Andrzej Stefański[1], Marian Wiercigroch[2] and Tomasz Kapitaniak[1]

[1]*Division of Dynamics, Technical University of Łódź, Stefanowskiego 1/15, 90-924 Łódź, Poland*
[2]*Centre for Applied Dynamics Research, School of Engineering, University of Aberdeen, King's College, Aberdeen AB24 8UE, UK*

In this paper, the phenomena of hysteretic behaviour of friction force observed during experiments are discussed. On the basis of experimental and theoretical analyses, we argue that such behaviour can be considered as a representation of the system dynamics. According to this approach, a classification of friction models, with respect to their sensitivity on the system motion characteristic, is introduced. General friction modelling of the phenomena accompanying dry friction and a simple yet effective approach to capture the hysteretic effect are proposed. Finally, the experimental results are compared with the numerical simulations for the proposed friction model.

Keywords: dry friction; hysteresis; modelling; experiment

1. Introduction

Modelling of dry friction has been the subject of active scientific research since Coulomb's hypothesis (Coulomb 1785). It appears in many, if not all, mechanical systems commonly met in engineering practice, including wheels, brakes, valves, cylinders, bearings, transmissions and others. Therefore, reliable predictions of their dynamic responses require robust dry friction models. In general, there are many different types of dry friction models and it is crucial to appropriately choose one that best suits the modelled problem. For example, if one considers the dynamics of a system where the relative velocity practically remains constant, there is no need for sophisticated dry friction models and even the simplest one described by the Coulomb law will suffice. However, the systems with dry friction can often exhibit more complex dynamical behaviour, such as chaotic or even stochastic responses (Den Hartog 1931; Tolstoi 1967; Shaw 1986; Popp & Stelter 1990; Wojewoda 1992; Feeny & Moon 1994; Wiercigroch 1994; Oestreich 1998; Bogacz & Ryczek 2003). Then, the chosen model must account for the transition from static to dynamic friction and should provide a means of guiding the system through zero relative velocity. Such a model should also describe hysteretic dynamical behaviour of dry friction arising from the

* Author for correspondence (jerzy.wojewoda@p.lodz.pl).

One contribution of 8 to a Theme Issue 'Experimental nonlinear dynamics I. Solids'.

pre-sliding displacement, the frictional lag or the non-reversibility of friction force, and other characteristic frictional phenomena like the Stribeck effect or the varying breakaway force. However, it is not easy to include all these frictional effects in a single model. It is especially difficult to define a mechanism governing the switch between the stick phase (pre-sliding) and the macroscopic sliding phase. Recently, several friction models including the above-mentioned properties have been suggested (Armstrong-Hélouvry 1991; Powell & Wiercigroch 1992; Armstrong-Hélouvry *et al.* 1994; Canudas de Wit *et al.* 1995; McMillan 1997; Liang & Feeny 1998*a*; Al-Bender *et al.* 2004); however, they are too complicated to be applied in practical engineering problems.

In this paper, we propose a simple approach to modelling of the hysteretic effects. A mathematical description of our model has been developed on the basis of experimental studies and other well-known friction characteristics. Its main advantage is a good approximation of the real nature of the friction force during macroscopic sliding motion of arbitrary type, i.e. regular, chaotic and stochastic responses. Thus, during the experimental studies, we have concentrated more on the pure sliding case (the oscillations with very short stops) rather than stick–slip motion.

The paper is organized as follows. In §2 the physical properties of the friction force are briefly described. Section 3 concerns a problem of friction modelling, which is exemplified by several existing friction models (static and dynamic). A description of the proposed model is presented in detail in §4. In §5 the experimental results and the numerical simulations performed using tested friction characteristic are compared. Section 6 contains the discussion and conclusions.

2. Friction phenomena

Friction force is a reaction in the tangential direction between a pair of contacting surfaces. Dry friction phenomenon can be treated as a result of various factors, i.e. physical properties of the material of frictional surfaces, its geometry and topology, relative velocity, and displacement of the bodies in contact.

The first description of dynamical behaviour of friction force, assuming that its constant value is independent of velocity, was formulated by Coulomb (1785). Newer experiments (from the beginning of the twentieth century) show nonlinear dependencies on the contact velocity rather than the constant one (see Stribeck 1902; Rabinowicz 1951). These experiments were often performed for stationary conditions, e.g. constant velocity. The friction force as a function of velocity for constant velocity motion is called the Stribeck curve (Stribeck 1902). Stribeck's work has shown a nonlinear transition from stick to slip. Therefore, the dip in friction force (figure 1*a*) observed at low values of the relative velocity is called the Stribeck effect. An interesting property of stick–slip transition is breakaway force (Rabinowicz 1951), i.e. the force required to stop sticking and initiate the motion. Experimental studies on the nature of static friction and the breakaway force led to the conclusion that the magnitude of this force depends on the rate of increase of the friction force during stick (Johannes *et al.* 1973). Faster increase results in smaller breakaway force (figure 8*b*). Hence, varying level of the breakaway force can also be identified as a function of dwell time, i.e. the time at zero velocity (figure 1*c*).

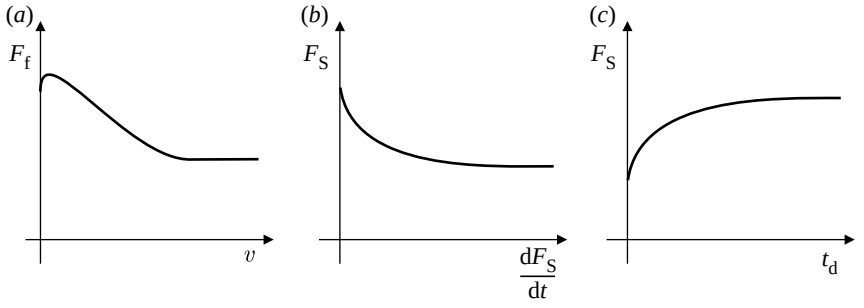

Figure 1. (*a*) Stribeck curve: friction force F_f versus velocity of the relative motion. (*b*,*c*) Breakaway force F_S a function of force rate dF_S/dt and dwell time t_d, respectively.

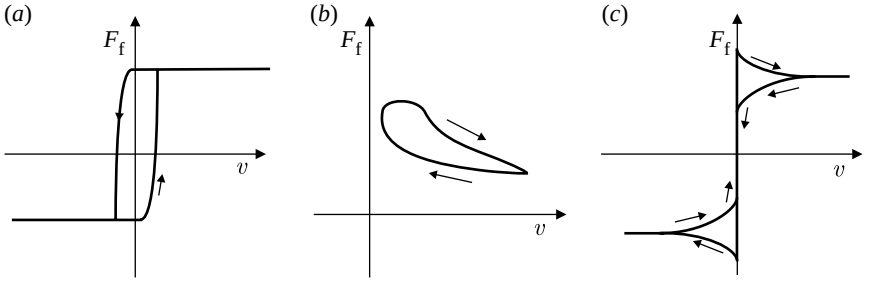

Figure 2. (*a*) Hysteretic effects of dry friction: contact compliance, (*b*) frictional memory and (*c*) non-reversible friction characteristic.

The next group of characteristic friction features are hysteretic effects accompanying frictional processes. One of them can appear during sticking and during the switch between stick and slip (slide) phases, and it is caused by the spring-like behaviour of the friction force before the actual sliding. This microscopic motion phenomenon, also called pre-sliding displacement, is caused by tangential stiffness between the bodies in contact (compliant contact; Courtney-Pratt & Eisner 1956; Harnoy & Friedland 1994; Liang & Feeny 1998*a*–*c*). Such contact compliance may arise from elastic deformation near the contact point or in the surrounding structure. Pre-sliding motion is represented by a narrow hysteresis around the zero relative velocity (figure 2*a*).

Another hysteretic effect can appear during oscillations with macroscopic sliding, i.e. periodic, relatively large-scale motion with pure sliding. Such phenomenon has been reported for the first time during experiments with a periodic relative velocity of unidirectional motion (see Hess & Soom 1990). The friction–relative velocity relationship obtained experimentally appeared as that shown in figure 2*b*. The hysteresis was observed as velocity varied. The size of the loop increases as the velocity variations become faster (Olsson *et al.* 1998). The friction force is lower for decreasing velocities than increasing velocities. Therefore, its dynamical behaviour is explained by the existence of frictional memory caused by a lag in the friction force. Similar hysteretic characteristics of friction can also be observed during regressive (two-way) oscillations with macroscopic sliding. Some experimental and analytical studies confirm the existence of different slopes of friction force for the acceleration and deceleration

phases (figure 2*c*; Den Hartog 1931; Bell & Burdekin 1970). This is called the non-reversibility of friction force (Powell & Wiercigroch 1992; Wiercigroch 1993; Wiercigroch *et al.* 1999).

3. Review of friction models

In general, there are two ways of describing friction, *static* and *dynamic* friction approach. The fundamental difference between them is in so-called frictional memory. For the static friction models, this frictional memory does not feature and is modelled as non-reversibility or described with frictional lag. Static models usually have a form of direct dependence between the friction force and the relative velocity. The dynamic friction models, where memory effect is described with a complementary dynamics between the velocity and the friction force, form an alternative approach. The main idea of such friction description is to introduce the state variables (or internal states) that determine the friction, where time evolution of state variables is given by an additional differential equation.

A practical engineering approach, indebted to Coulomb, simplifies the friction force to a constant value opposite to the relative velocity of the contacting bodies

$$F_{\mathrm{f}} = Nf_{\mathrm{C}}\,\mathrm{sign}(v), \tag{3.1}$$

where F_{f} is the friction force; N is the normal load; f_{C} is the coefficient of Coulomb friction; and v is the relative velocity. This is the simplest static model of friction. Such a force takes two values with equal size amplitude but opposite in sign. This classical friction model does not explain all dynamical behaviour observed in mechanical systems with friction. For example, the mathematical model of self-excited vibrations, induced by dry friction, requires a non-zero slope of friction characteristic in order to initialize such kind of oscillations (Babakov 1968). Another disadvantage of the Coulomb characteristic is the lack of physical interpretation of friction in the neighbourhood of zero relative velocity. However, such a simplified friction model is often used in engineering applications, as it gives the first approximation.

Nonlinear friction characteristics, including the Stribeck effect, are better approximations of real characteristics of friction. In such case, the classical Coulomb model of constant kinetic friction (equation (3.1)) becomes

$$F_{\mathrm{f}} = Nf_{\mathrm{C}}\left(1 + \frac{f_{\mathrm{S}} - f_{\mathrm{C}}}{f_{\mathrm{C}}}\,g(v)\right)\mathrm{sign}(v), \tag{3.2}$$

where f_{S} is the coefficient of static friction and $g(v)$ is a nonlinear function describing a characteristic of the Stribeck curve. Typical descriptions of the relationship between friction force and relative velocity are as follows:

(i) exponential (Tustin 1947)

$$\exp(-|v|/v_{\mathrm{S}}), \tag{3.3}$$

(ii) generalized exponential (Bo & Pavelescu 1982)

$$\exp\,-\alpha|v|^{\delta}, \tag{3.4}$$

(iii) Gaussian (Armstrong-Hélouvry 1991)

$$\exp\ -(v/v_S)^2, \tag{3.5}$$

(iv) Laurentzian (Hess & Soom 1990)

$$\frac{1}{1+(v/v_S)^2}, \quad \text{and} \tag{3.6}$$

(v) Popp–Stelter (Popp & Stelter 1990)

$$\frac{1}{1+\eta_1|v|}+\frac{\eta_2 v^2}{f_S-f_C} \tag{3.7}$$

where α, δ, η_1 and η_2 are constants and v_S is the Stribeck velocity, i.e. a boundary value of relative velocity between the microslip (stick) and the macroslip.

It is worth pointing out here that modelling of the hysteretic effects connected with the contact compliance or frictional memory requires even more sophisticated friction models. A simple static approach to modelling of the hysteretic behaviour of friction force during macroscopic sliding has been proposed by Powell & Wiercigroch (1992) and Wiercigroch *et al.* (1999). Their idea is based on the non-reversible friction characteristic. A symmetrical (with respect to the coefficient of Coulomb friction f_C, figure 2*c*) case of non-reversible friction characteristic can be modelled by equation (3.2), with the following form of nonlinear function including the sign of relative acceleration $\dot{v}$:

$$g(v) = \exp(-\alpha|v|)\mathrm{sign}(v\dot{v}). \tag{3.8}$$

Another example of a well-known approach is the *seven-parameter model*, which can be described as the static model of the hysteretic behaviour (see Armstrong-Hélouvry 1991; Armstrong-Hélouvry *et al.* 1994). It is even more complicated than the non-reversible friction characteristic because it actually consists of two separate models: one for sticking phase and the other for sliding phase. When sticking, the friction is described by the linear spring model:

$$F_f(x) = k_s x, \tag{3.9}$$

where k_s is the contact stiffness to account for pre-sliding displacement. During sliding, the friction is modelled as Coulomb (F_C) and viscous damping (F_v) with the Stribeck effect and frictional memory:

$$F_f(v,t) = \left[F_C + F_v|v| + F_S(\gamma, t_d)\frac{1}{1+(v(t-\tau)/v_S)^2}\right]\mathrm{sgn}(v), \tag{3.10}$$

where $F_S(\gamma,t_d)$ denotes the varying friction level at the breakaway, which depends on an empirical parameter γ and the dwell time t_d, and τ is the time delay introduced to model a hysteretic effect of frictional memory. A major problem experienced during numerical implementation of such static models is to simulate the stick–slip transitions, i.e. to define a mechanism governing the switch between equations (3.9) and (3.10).

In classical meaning, the static models have a form of static relationships (maps) between the friction force and the velocity only. However, the static models can also map the friction force as a function of acceleration (apart from

the relative velocity). For the first time, it was proposed by Hunt *et al.* (1965) that the friction force is dependent on another variable besides velocity, i.e. acceleration. Another example of a similar approach was given by McMillan (1997). Stefański *et al.* (2003) also suggested a friction model where the current value of relative acceleration should be used. This model was elaborated on the basis of non-reversible friction characteristic (equations (3.2) and (3.8)). The function $g(v)$ in this model is described by the formula

$$g(v) = \exp\left(-\frac{a_1|v|}{|\dot{v}| + a_2}\right)\mathrm{sgn}(v\dot{v}), \tag{3.11}$$

where a_1 and a_2 are constants. Such models allow us to model the hysteretic frictional memory effect, because an appearance of acceleration in the description of friction characteristic can be treated as a result of the time delay in velocity.

Better approximations of the hysteretic dynamical behaviour of the friction force have facilitated the development of dynamic friction models. The first approach that can be classified as a dynamic friction model was proposed by Dahl (1968). It uses the stress–strain curve known from classical solid mechanics (Ramberg & Osgood 1943)

$$\frac{\mathrm{d}F_\mathrm{f}}{\mathrm{d}x} = k_\mathrm{s}\left(1 - \frac{F_\mathrm{f}}{F_\mathrm{C}}\mathrm{sgn}(v)\right)^{\alpha}, \tag{3.12}$$

where k_s is the stiffness coefficient and α determines the shape of the stress–strain curve. Introducing $F_\mathrm{f} = k_\mathrm{s} z$ for $\alpha = 1$, the model can be rewritten as

$$\begin{cases} \dfrac{\mathrm{d}z}{\mathrm{d}t} = v - \dfrac{k_\mathrm{s}|v|}{F_\mathrm{C}}z, \\ F_\mathrm{f} = k_\mathrm{s} z, \end{cases} \tag{3.13}$$

where z is the internal state variable. Equation (3.12) exemplifies a dynamic generalization of the classical Coulomb friction. However, this approach does not model the Stribeck effect and the static friction. These are the main motivations for further extensions of the Dahl model.

Recently, several more dynamic models have been proposed (Haessig & Friedland 1991; Bliman & Sorine 1995; Canudas de Wit *et al.* 1995). An example of these approaches is the LuGre model, which is related to the bristle interpretation of friction by Bliman & Sorine (1995). The model is formulated as follows:

$$\begin{aligned} \frac{\mathrm{d}z}{\mathrm{d}t} &= v - k_\mathrm{s}\frac{|v|}{g(v)}z \quad \text{and} \\ F_\mathrm{f} &= k_\mathrm{s} z + c_\mathrm{s}\frac{\mathrm{d}z}{\mathrm{d}t} + cv, \end{aligned} \tag{3.14}$$

where the internal state variable z denotes the average bristle deflection; the coefficients k_s and c_s define the bristles stiffness and the bristles damping, respectively; cv is the viscous friction; and the function $g(v)$ models the Stribeck effect according to equation (3.5). An advantage of the LuGre model is its rich dynamic behaviour giving possibilities to model stick–slip transitions, varying breakaway force, frictional memory and hysteretic effects, and the Stribeck curve. The model by Al-Bender *et al.* (2004) can be qualified as an upgrade of the LuGre model.

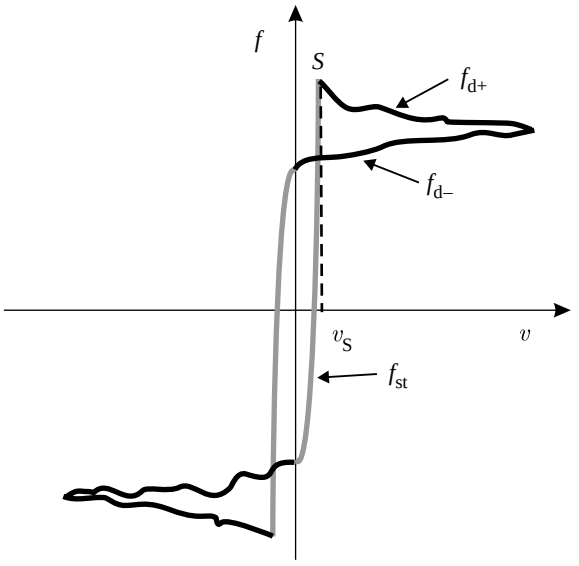

Figure 3. Example of dry friction characteristic described by equations (4.2)–(4.4) generated during one cycle of oscillation. The perturbations of the characteristic's curves due to a stochastic component are visible.

It can often happen that even the most sophisticated friction model does not fully reflect the friction characteristics generated experimentally due to the influence of some random factors (e.g. variations of normal pressure force or inhomogeneous asperity of contacting surfaces). Modelling such factors can be realized by the introduction of a stochastic component (e.g. Hinrichs *et al.* 1998).

Concluding this short review of friction models, we can state that most static models (equations (3.1)–(3.8)) usually give only the first approximation. In particular, they do not describe accurately the transitions from stick to slip and vice versa. But their advantage lies in simplicity and applicability in numerical simulations. The dynamic friction approaches (equations (3.12)–(3.14)) and some more advanced static models (equations (3.9) and (3.10)) allow one to model precisely most of the observed frictional phenomena, but they are usually complex and hard to implement.

4. Adopted dry friction model

The conclusion from §3 motivated us to elaborate a new proposal of dry friction model. Our main intention was to formulate a model that incorporates two features: it should be easy to implement in numerical calculations and it should model friction phenomena with high precision, as described in §2. Taking into consideration the discussion on friction modelling presented in §3, we decided to propose a static model of the hysteretic type, which is enriched with a stochastic component. A typical realization of such characteristic is depicted in figure 3.

Its mathematical description can be generalized to the following form:

$$f(v,\dot{v}) = \begin{cases} f_{\mathrm{st}}\,\mathrm{sgn}(v) \text{ for } f_{\mathrm{st}} < f_{\mathrm{d}+} \text{ and } \mathrm{sgn}(v\dot{v}) > 0, \\ f_{\mathrm{d}+}\,\mathrm{sgn}(v) \text{ for } f_{\mathrm{st}} > f_{\mathrm{d}+} \text{ and } \mathrm{sgn}(v\dot{v}) > 0, \\ f_{\mathrm{d}-}\,\mathrm{sgn}(v) \text{ for } \mathrm{sgn}(v\dot{v}) < 0, \end{cases} \tag{4.1}$$

where

$$f_{\mathrm{st}} = \frac{1}{2}\frac{k_{\mathrm{s}}}{N}\frac{v^2}{|\dot{v}|} - f_0, \tag{4.2}$$

$$f_{\mathrm{d}+} = f_{\mathrm{C}}\left[1 + \frac{f_{\mathrm{S}}(v) - f_{\mathrm{C}}}{f_{\mathrm{C}}}\left(g(v,\dot{v}) + f_{\mathrm{R}}(x,v)\right)\right] \tag{4.3}$$

and

$$f_{\mathrm{d}-} = f_{\mathrm{C}}\left[1 - \frac{f_{\mathrm{S}} - f_{\mathrm{C}}}{f_{\mathrm{C}}}\left(g(v,\dot{v}) + f_{\mathrm{R}}(x,v)\right)\right]. \tag{4.4}$$

Equation (4.2) describes a friction coefficient f_{st} during the compliant contact (grey curves in figure 3) and equations (4.3) and (4.4) the dynamic friction coefficient in acceleration ($f_{\mathrm{d}+}$) and deceleration ($f_{\mathrm{d}-}$) phases, respectively (black curves in figure 3). The general characteristic of the friction model given by equations (4.2)–(4.4) allows an arbitrary form of the function g and modelling of the Stribeck effect (e.g. one of the formulae given by equations (3.3)–(3.8) or (3.11)). The random factors appearing during the friction process are simulated with stochastic function f_{R} which can also be generated using various classical random or semi-random processes. Owing to the experimental observation (see §5), we have included random (stochastic) component only in the formulae for kinetic friction coefficient (equations (4.3) and (4.4)). For the considered cases of sliding motion, the friction force exhibits regular behaviour in compliant contact phase (figures 8*a*–11*a*).

(*a*) *Pre-sliding hysteresis and breakaway force*

First, we consider a classical case (Armstrong-Hélouvry *et al.* 1994; Liang & Feeny 1998*a*) of spring-like behaviour of the friction force during stick phase, as shown in figure 4. Hence, this static force is $F_{\mathrm{f}} = F_{\mathrm{st}} = k_{\mathrm{s}}z$ and its time derivative is $\mathrm{d}F_{\mathrm{st}}/\mathrm{d}t = k_{\mathrm{s}}\mathrm{d}z/\mathrm{d}t$, where k_{s} is the contact stiffness and z is an internal variable (figure 4). Let us assume that x is the relative displacement, so $v = \mathrm{d}x/\mathrm{d}t$. While sticking, the relative velocity of the frictional damper surfaces $w = \mathrm{d}x/\mathrm{d}t - \mathrm{d}z/\mathrm{d}t$ is equal to zero; hence, $\mathrm{d}x/\mathrm{d}t = \mathrm{d}z/\mathrm{d}t$ and

$$\frac{\mathrm{d}F_{\mathrm{st}}}{\mathrm{d}t} = \frac{\mathrm{d}F_{\mathrm{st}}}{\mathrm{d}v}\frac{\mathrm{d}v}{\mathrm{d}t} = k_{\mathrm{s}}\frac{\mathrm{d}x}{\mathrm{d}t} \Rightarrow \frac{\mathrm{d}F_{\mathrm{st}}}{\mathrm{d}v} = k_{\mathrm{s}}\left(\frac{\mathrm{d}v}{\mathrm{d}t}\right)^{-1} v. \tag{4.5}$$

Rearranging and integrating equation (4.5) leads to

$$F_{\mathrm{st}} = \frac{1}{2}k_{\mathrm{s}}\left(\frac{\mathrm{d}v}{\mathrm{d}t}\right)^{-1} v^2 - F_0, \tag{4.6}$$

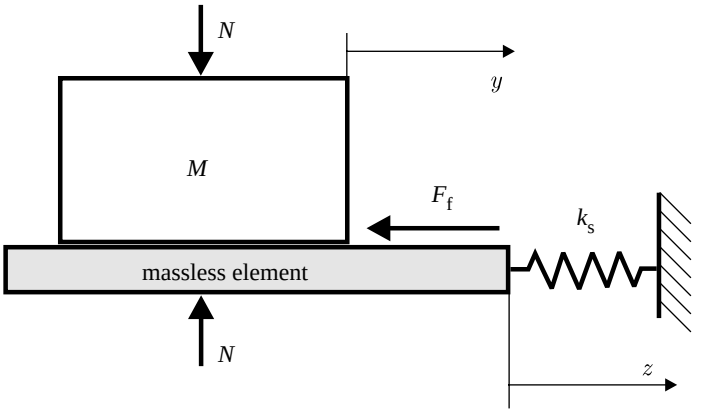

Figure 4. Model of dry friction damper with the contact compliance.

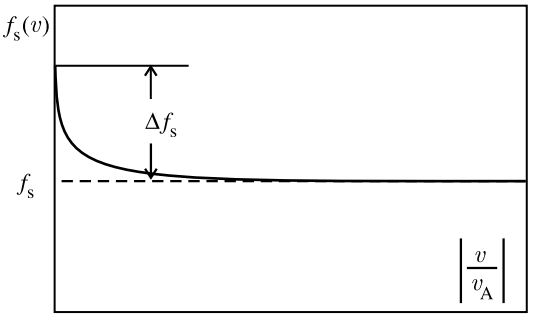

Figure 5. Function modelling varying level of the breakaway force (equation (4.7)).

where F_0 is an initial value of F_{st} for $v=0$. Equation (4.2) is obtained by substituting $F_{st}=Nf_{st}$, where N is the normal force and $f_0=f_{d-}(v=0)=F_0/N$ represents a value of the friction coefficient corresponding to F_0.

It is worth noting that f_0 can take various values during each transition through the zero relative velocity. An intersection of f_{st} and f_{d+} curves (point S in figure 3), where a transition from stick to slip takes place, determines a value of the Stribeck velocity v_S and the varying level of the breakaway force. To model typical characteristics of the breakaway force (figure 1*b*), we applied a non-constant value of f_S. From equation (4.5), it is easy to see that a varying level of the breakaway force is a function of velocity during stick phase, $F_S=h(v)$. Hence, the breakaway coefficient can be approximated by the formula

$$f_S(v) = f_S + \Delta f_S \frac{1}{1+\left|\frac{v}{v_A}\right|}, \tag{4.7}$$

where Δf_S determines a range of the breakaway force variation (figure 5) and v_A is an adjusting parameter representing an average value of the Stribeck velocity, i.e.

$$v_A \approx 0.5 v_S^{\max}. \tag{4.8}$$

An illustration of equation (4.7) shown in figure 5 confirms that this function is a good reflection of the experimental observations (figure 1*b*). The numerical analysis carried out has shown that dependence of the breakaway coefficient on the dwell time also has a similar characteristic to the function, as shown in figure 1*c*.

(b) Frictional memory

Frictional memory during the slip phase is modelled in equations (4.3) and (4.4) by the function g, including the relative acceleration $\dot{v}$, which can be related to the time delay τ of the relative velocity, as $v(t-\tau) \approx v(t) - \tau\dot{v}$. Thus, the effect of frictional memory can be obtained by applying a delay in velocity for the chosen form of function g, i.e. $g(v(t-\tau))$ instead of $g(v(t))$ in equations (3.2)–(3.8), or any other friction characteristic that includes the relative acceleration (e.g. equation (3.11)).

(c) Non-reversibility

This effect is modelled by signs '+' and '−' in quadratic brackets of equations (4.3) and (4.4), respectively. Earlier experiments and analyses show (Powell & Wiercigroch 1992; Wojewoda 1992; Wojewoda *et al.* 1993; Wiercigroch *et al.* 1999; Stefański *et al.* 2001, 2003) that the non-reversibility of dry friction becomes significantly visible during the pure sliding with a relatively large amplitude of relative velocity.

(d) Stochastic effects

In our studies, the stochastic component of the friction force has been expressed as that shown by Wiercigroch & Cheng (1997). We assume that the roughness of the sliding elements is described as a stationary Gaussian process. Hence, it is reasonable to model the fluctuations of the friction force, also by the description of a stationary Gaussian process. In general, this process is three-dimensional (equation (4.8)). However, in this paper, we consider the stochastic component of the friction force f_{R} as a one-dimensional process $f(v)$.

It is assumed that the stochastic component of the friction force f_{R} has been normalized, so that the mean is equal to 1:

$$\bar{f} = \lim_{v \to v_{\max}} \frac{1}{v - v_{\min}} \int_{v_{\min}}^{v} f(v)\mathrm{d}v = 1, \tag{4.9}$$

where $f(v)$ is the specific (normalized) stochastic component of the friction force. It is characterized by the standard deviation σ and autocorrelation coefficient $R(z)$, where z is the distance separating the two points. A power spectral density function $S(\omega)$ is defined by

$$S(\omega) = \frac{1}{2\pi} \int_{-\infty 0}^{\infty} R(v)\mathrm{e}^{\mathrm{i}\omega v}\,\mathrm{d}v. \tag{4.10}$$

The autocorrelation coefficient is typically characterized by a correlation length, say L_{c}, which is related to the distance beyond which the correlation of the velocity fluctuation diminishes. The correlation length and the form of the autocorrelation function should be determined experimentally either by direct testing of the process or by an interpretation of the vibration signal. Unfortunately, no such measurements are available to our knowledge.

As a first-cut approximation, a simple but popular model for the autocorrelation coefficient is adopted for the present study,

$$R(z) = \mathrm{e}^{\lambda|v|}. \tag{4.11}$$

Here, $1/\lambda$ characterizes the correlation length. The power spectral density function corresponding to equation (4.11) is

$$S(\omega) = \frac{1}{\dot{\pi}(\lambda^2 + \omega^2)}. \tag{4.12}$$

With the above statistical quantities, it is possible to generate artificially a random signal with the same statistics. The technique adopted is the spectral representation method (Shinozuka & Jan 1972; Shinozuka & Deodatis 1992). It is modelled by the series

$$f_{\mathrm{R}}(v) = 2\sigma \sum_{k=0}^{N-1} \sqrt{S(\omega_k)\Delta\omega}\, \cos(\omega_k v + \phi_k), \tag{4.13}$$

where σ is the standard deviation; ϕ_k is a random phase angle uniformly distributed over $[0,2\pi]$; $\omega_k = k\Delta\omega$; and $\Delta\omega$ is the frequency increment.

In summary, our dry friction model allows us to simulate various frictional phenomena, i.e. contact compliance, frictional memory, non-reversibility, varying breakaway force, Stribeck effect and influence of random factors. From the point of view of practical application, the presented approach can be classified as a static friction model. In its general form, it consists of five constant parameters Δf_{S}, f_{S}, f_{C}, k_{s} and v_{A}; one varying parameter f_0; and the stochastic component f_{R} with standard deviation σ. Additionally, the pressure force N appears in the description of the stick phase.

5. Experimental and numerical studies

(*a*) *Experimental rig*

The experimental oscillator designed by Wiercigroch *et al.* (1999), as shown in figure 6*a*, comprises a block mass that oscillates along two guiding posts being supported with two coil springs, with a second mass consisting of a vertical plate (tongue) introducing dry friction to the system. The tongue is a vertically positioned steel plate mounted to a force transducer (FT) connected to the vibrating mass. This plate is in contact with two changeable frictional pads connected through a clamping mechanism to the base. A pneumatic actuator under constant air pressure is to supply constant level of force acting on the clamping mechanism, which presses both pads against the tongue. The design allows for self-fitting of the friction elements to two swivel blocks housing the friction plates mounted on their slots using ball links. This helps compensate any misalignment of clamping while in oscillation. For measuring the relative velocity of the oscillating mass, a linear velocity transducer was used. The complete rig was mounted on the top of an electrodynamic shaker. The base excitation provided by the shaker was controlled by a data acquisition system.

The rig was excited around its resonance frequency in the range between 5 and 25 Hz. Discrete time series of the data were recorded. The data acquisition system also allowed for control of the input signals. In this way an arbitrary wave could be used as system excitation, which proved to be beneficial as multi-frequency periodic waves were much more useful in the identification of the system parameters.

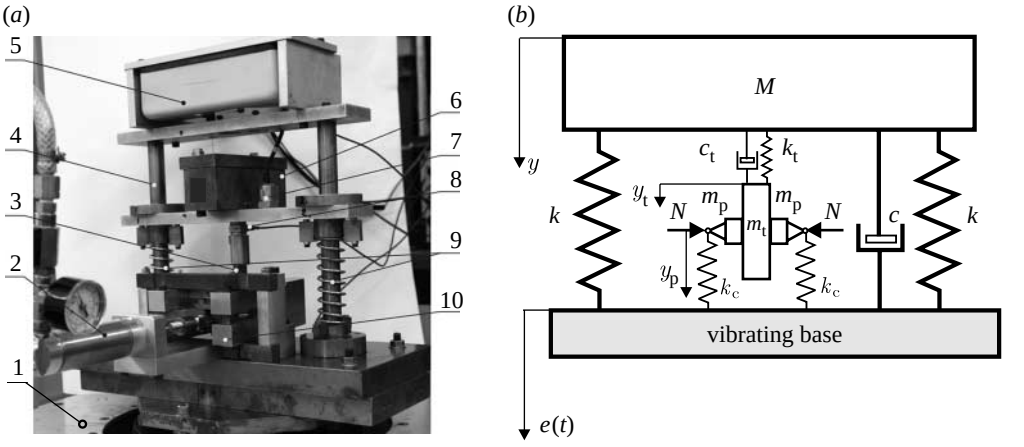

Figure 6. (*a*) General view of the experimental rig (Wiercigroch *et al.* 1999): 1, shaker; 2, pneumatic actuator with gauge; 3, friction tongue; 4, guiding post; 5, case of the linear velocity transducer (LVT) and linear velocity and displacement transducer (LVDT); 6, main mass; 7, accelerometer; 8, force transducer; 9, coil springs; 10, clamping mechanism. (*b*) Physical model of the experimental rig: M, oscillating mass (kg); m_t, mass of the tongue (kg); m_p, mass of the friction pads (kg); k, stiffness of the coil springs ($\mathrm{N\,m^{-1}}$); c, effective viscous damping of the oscillator ($\mathrm{Ns\,m^{-1}}$); k_c, compliance of pads ($\mathrm{N\,m^{-1}}$); k_t, stiffness of the tongue ($\mathrm{N\,m^{-1}}$); c_t, effective viscous damping between the tongue and FT ($\mathrm{N\,m^{-1}}$).

(*b*) *Experimental measurements*

In our experimental studies, direct measurements of friction force were performed by means of a FT, which is located between the main mass and the frictional tongue. However, the signal obtained from the FT does not fully reflect the actual friction force. The main reason for this is that the FT senses all forces including the inertia generated in the system. Another possible reason is that the friction and system dynamics cannot be decoupled due to a finite compliance of the sensing element (FT; Liang & Feeny 1998*c*; Lampaert *et al.* 2004).

Therefore, we determined the friction force indirectly on the basis of a simplified mathematical model of the rig given by equation (5.2). According to equation (5.3), an indirect estimation of the rig friction force requires a knowledge of three signals and three parameters of the frictional system. The values of the relative displacement x and the relative velocity v were measured directly by the LVDT and LVT transducers, respectively. The accelerometer connected to the main vibrating mass gave the acceleration signal $\ddot{y}$. The total mass (with frictional tongue) of the oscillating part amounts to $M=3.35$ kg, the stiffness of supporting springs is $2k=5040\ \mathrm{N\,m^{-1}}$ and the effective viscous damping coefficient applied in calculations was estimated as $c=16.85\ \mathrm{Ns\,m^{-1}}$. This coefficient was identified according to the method described by Liang & Feeny (1998*b*), which allows separation of Coulomb and viscous friction.

During the experiment, constant air pressure of $p=1$ bar was applied to the clamping mechanism. Various forms of base excitation were provided to the oscillator: harmonic, multi-periodic and non-periodic.

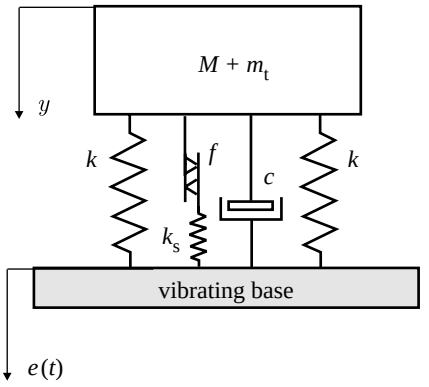

Figure 7. Simplified model of dry friction oscillator.

(*c*) *Numerical modelling*

For the physical model of the friction oscillator depicted in figure 6*b*, the following 3-d.f.s mathematical model has been formulated:

$$\left.\begin{aligned} M\ddot{y} &= -2k[y-e(t)]-c[\dot{y}-\dot{e}(t)]-k_{T1}(y-y_t)-c_{T1}(\dot{y}-\dot{y}_t),\\ m_t\ddot{y}_t &= -k_{T1}(y_t-y)-c_{T1}(\dot{y}_t-\dot{y})-F_f(v)\\ \text{and}\\ 2m_p\ddot{y}_p &= -2k_c[y_p-e(t)]+F_f(v), \end{aligned}\right\} \tag{5.1}$$

where y, y_t and y_p are absolute displacements of the main mass, tongue and pads, respectively, and $e(t)$ is the displacement of the base.

The detailed description of the parameters can be found in figure 2*b*. Unfortunately, from a viewpoint of the indirect measurement of friction force, formulae (5.1) are not useful due to a number of unknown parameters related to the pads and tongue motion. Therefore, we reduced the 3-d.f.s to a single d.f. system with the dominant degree of freedom represented by the coordinate y. A simplified scheme of the experimental rig is shown in figure 7. In order to realize such a simplification, we have removed the FT and substituted the compliance of pads $2k$ with contact stiffness k_s. Now, the dynamics of this system can be described by the following second-order differential equation:

$$(M+m_t)\ddot{y} = -2k[y-e(t)]-c[\dot{y}-\dot{e}(t)]-F_f. \tag{5.2}$$

The subtractions $y-e(t)$ and $\dot{y}-\dot{e}(t)$ are relative displacement x and relative velocity v between the oscillating mass and the base, respectively. Thus, we can determine the friction force F_f from experimental data as

$$F_f = -[(M+m_t)\ddot{y}+2kx+cv]. \tag{5.3}$$

For the needs of numerical simulations, equation (5.2) is rewritten in the form of two first-order differential equations

$$\left.\begin{aligned} \dot{y}_1 &= y_2\\ \text{and}\\ \dot{y}_2 &= -\frac{1}{M+m_t}\{2k[y_1-e(t)]-c[y_2-\dot{e}(t)]-Nf(v)\}, \end{aligned}\right\} \tag{5.4}$$

where $y_1 = y$, $y_2 = \dot{y}$ and $v = y_2 - \dot{e}(t)$ and N is the normal force.

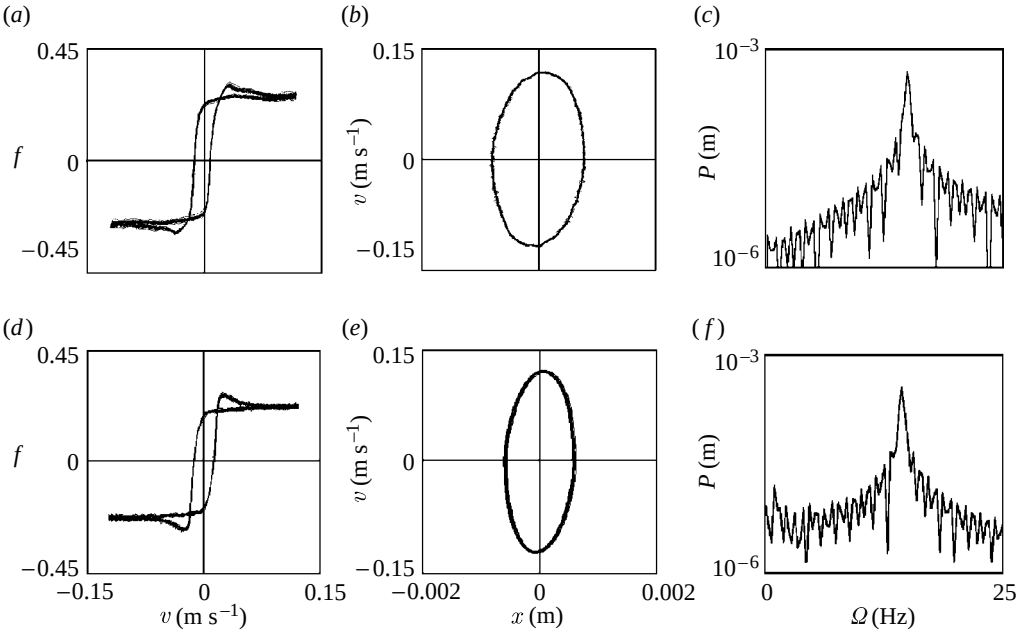

Figure 8. Comparison of (*a–c*) experimental and (*d–f*) numerical results for the simple periodic motion. (*a,d*) Friction characteristics, (*b,e*) phase portraits and (*c,f*) power spectra.

The parameters of the oscillator were determined from the experimental investigations. Various excitations $e(t)$ were applied in numerical simulations. Periodic (the cases shown in figures 8*d–f* and 9*d–f*) or quasi-periodic driving (figure 10*d–f*) was modelled. Irregular driving (the case depicted in figure 11*d–f*) was realized using a chaotic signal generated from the Duffing oscillator: $\ddot{q}+0.1\dot{q}-10^4q(1-q^2)=a\cos(90t)$. We assumed a mean value of the pressure force $N=35\,\mathrm{N}$ corresponding to the experimental pressure of $p=1\,\mathrm{bar}$ (Wiercigroch *et al.* 1999).

In the numerical simulation, the model given by equation (5.4) and the friction characteristics (equations (4.1)–(4.4)) were used. The nonlinear function $g(v,\dot{v})$ appearing in equations (4.3) and (4.4) was applied in the following form:

$$g(v,\dot{v})=\frac{1}{1+\left(\frac{v-\tau\dot{v}}{v_\mathrm{A}}\right)^2}. \tag{5.5}$$

The current approach can be treated as the development of the friction characteristic given by equation (3.6), where a delay is taken into account. v_A denotes an average Stribeck velocity as in equation (4.8), whereas the function describing the static coefficient of friction (equation (4.2)) has a form

$$f_\mathrm{st}=\frac{1}{2}\frac{k_\mathrm{s}}{N}\frac{v^2}{|\dot{v}|}-(2f_\mathrm{C}-f_\mathrm{S}), \tag{5.6}$$

where $f_0=2f_\mathrm{C}-f_\mathrm{S}$. The parameters of the friction model are $v_\mathrm{A}=0.02\,\mathrm{m\,s^{-1}}$, $f_\mathrm{S}=0.32$, $f_\mathrm{C}=0.25$, contact stiffness $k_\mathrm{s}=10^6\,\mathrm{N\,m^{-1}}$, time delay $\tau=0.002\,\mathrm{s}$ and

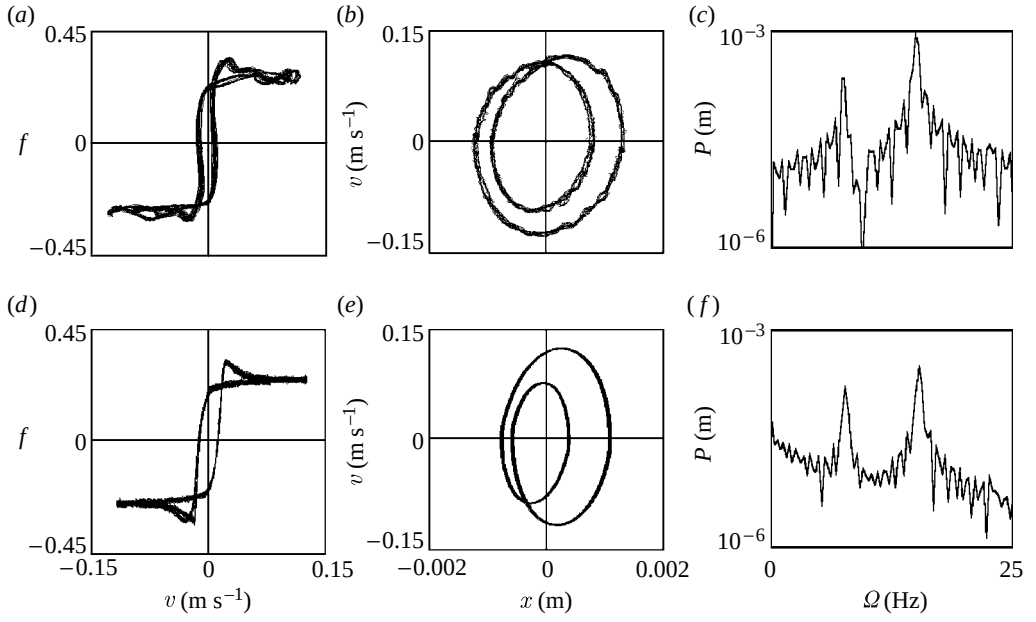

Figure 9. Comparison of (*a–c*) experimental and (*d–f*) numerical results for a multi-periodic motion. (*a,d*) Friction characteristics, (*b,e*) phase portraits and (*c,f*) power spectra.

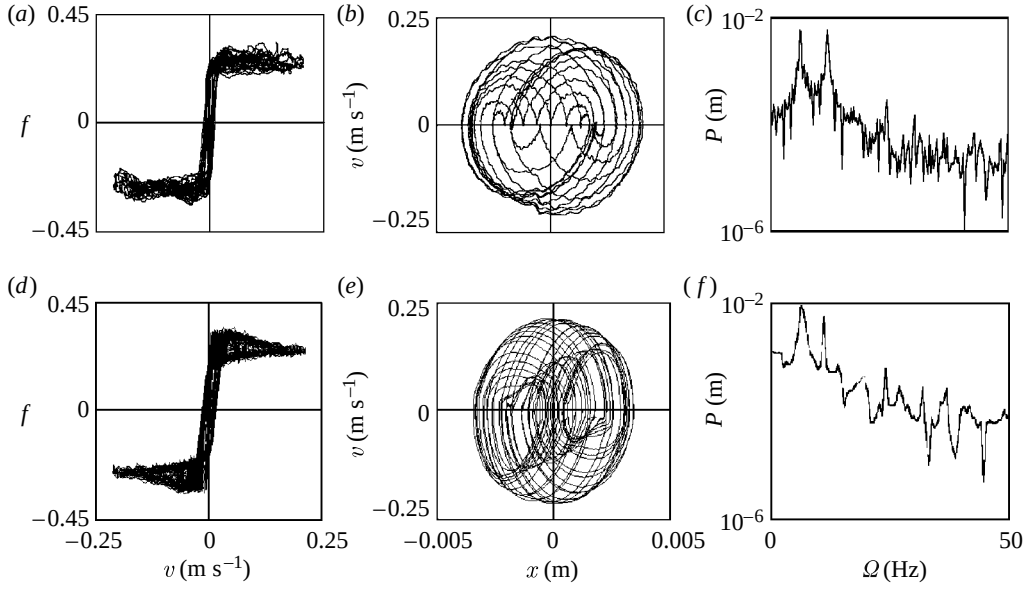

Figure 10. Comparison of (*a–c*) experimental and (*d–f*) numerical results for a quasi-periodic motion. (*a,d*) Friction characteristics, (*b,e*) phase portraits and (*c,f*) power spectra.

$\Delta f_S = 0.03$. These values were estimated from the experimental data. The stochastic component in equation (4.13) was applied with a value of standard deviation $\sigma = 0.05$.

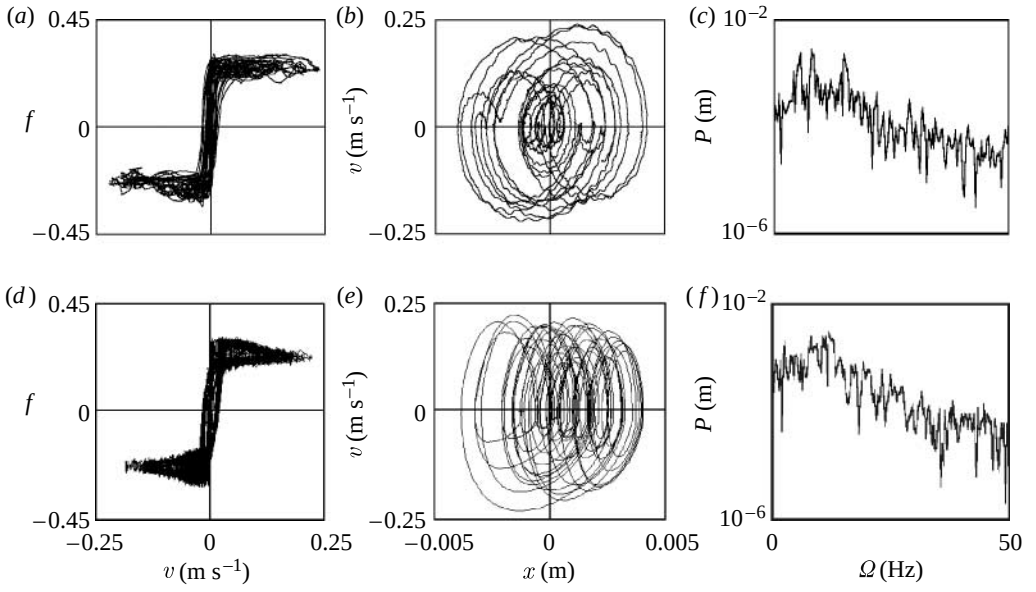

Figure 11. Comparison of (*a–c*) experimental and (*d–f*) numerical results for an irregular motion. (*a,d*) Friction characteristics, (*b,e*) phase portraits and (*c,f*) power spectra.

(*d*) *Experiments versus numerical simulations*

Figures 8*a–c* to 11*a–c* present the experimental results, whereas numerical simulations are shown in figures 8*d–f* to 11*d–f*. In each row, the friction characteristics, phase portrait and power spectrum are presented from left to right.

In the case shown in figure 8*a–c*, the friction oscillator was excited by a stationary harmonic driving. The response is almost harmonic (a regular ellipsoidal loop on the phase space (figure 8*b*) and one dominant peak in the frequency spectrum (figure 8*c*)). Figures 9*a–c* to 11*a–c* illustrate the results of the experimental studies for the multi-periodic and non-periodic excitations. The characteristic of these responses is confirmed by the corresponding frequency spectra. For the regular periodic or quasi-periodic motion, two dominant peaks can be distinguished (figures 9*c* and 10*c*). On the other hand, in the case of irregular response, the frequency spectrum is more continuous with a few smaller peaks (figure 11*c*).

The comparison of phase portraits (figures 8*b*–11*b*) with the corresponding friction characteristics from figures 8*a*–11*a* shows that if the motion of the system becomes more complex, then this is also reflected in the friction characteristics. Examining closely the phase portraits, we can observe one or two loops of the friction characteristic for the regular periodic responses (figures 8*a* and 9*a*) or countless number of such loops for the quasi-periodic (figure 10*a*) or non-periodic (figure 11*a*) motion of the oscillator. Another common feature of the experimentally generated friction characteristics is a clearly visible double hysteretic effect. The horizontal (central) part of hysteresis is caused by the contact compliance during pre-sliding motion, whereas the vertical branches are the effects of frictional memory.

As can be seen from this section, the experimental results shown in figures 8 to 11*a–c* correspond well to the numerical predictions shown in figures 8 to 11*d–f* for various qualitative responses of our frictional oscillator. This is due to the fact that the proposed model of friction apart from the aspect of non-reversibility caters for the stochastic nature of the interactions between the frictional pads and the tongue.

6. Concluding remarks

Experimental, numerical and theoretical analyses presented in this paper were focused on various phenomena accompanying the dry friction processes, including hysteretic effects caused by the frictional memory or contact compliance, varying breakaway force and Stribeck effect. These phenomena show the complexity and difficulty of friction description and modelling. In order to gain a further insight, we have proposed an alternative friction classification. Namely, the friction characteristics can be divided into two groups: (i) *insensitive* and (ii) *sensitive* to the system dynamics.

We concluded that the sensitivity is caused by the frictional memory and the varying level of the breakaway force. In the case of steady-state motion, these factors have no influence on the friction force and the behaviour can be explained with classical Coulomb or Stribeck models. The appearance of a hysteresis loop on the friction characteristic (figure 8*a*,*d*) is due to the presence of frictional memory; the level of the breakaway force is the same in each cycle of motion due to the constant dwell time. A significant difference between both groups of friction models can appear if motion of the system is more complex (multi-periodic, quasi-periodic, chaotic and stochastic).

On the basis of the analysis carried out for a dry friction oscillator, we have proposed a general friction model (equations (4.1)–(4.4)). The main advantage of this model is its simplicity for numerical simulations. This is a static friction model that depends only on several parameters, and assumed nonlinear friction function $g(v, \dot{v})$. Moreover, this approach enables one to simulate various frictional phenomena, including contact compliance, frictional memory, non-reversibility, varying breakaway force and Stribeck effect.

The comparisons between numerical (figures 8*d–f* to 11*d–f*) and experimental results (figures 8*a–c* to 11*a–c*) confirm that the proposed dry friction model is a good approximation of the observed frictional phenomena. However, it should be pointed out that the proposed model is valid for large macroscopic sliding. A precise description of microscopic sliding and stick–slip phenomena requires a further development.

This study was supported by the Polish Department for Scientific Research (DBN) under project no. NN 501 0710 33 and the University of Aberdeen.

References

Al-Bender, F., Lampaert, V. & Swevers, J. 2004 A novel generic model at asperity level for dry friction force dynamics. *Tribol. Lett.* **16**, 81–93. (doi:10.1023/B:TRIL.0000009718.60501.74)

Armstrong-Hélouvry, B. 1991 *Control of machines with friction*. Hingham, MA: Kluwer Academic Press.

Armstrong-Hélouvry, B., Dupont, P. & Canudas de Wit, C. 1994 A survey of models, analysis tools and compensation methods for the control of machines with friction. *Automatica* **30**, 1083–1138. (doi:10.1016/0005-1098(94)90209-7)

Babakov, I. M. 1968 *Theory of vibrations*. Moscow, Russia: Nauka. [In Russian.]

Bell, R. & Burdekin, M. 1970 A study of stick–slip motion of machine tool feed drives. *Proc. Inst. Mech. Eng.* **184**, 543–557.

Bliman, P.-A. & Sorine, M. 1995 Easy-to-use realistic dry friction models for automatic control. In *Proc. 3rd European Control Conference, Rome, Italy*, pp. 3788–3794.

Bo, L. C. & Pavelescu, D. 1982 The friction–speed relation and its influence on the critical velocity of stick–slip motion. *Wear* **82**, 277–289. (doi:10.1016/0043-1648(82)90223-X)

Bogacz, R. & Ryczek, B. 2003 Frictional phenomena in dynamical systemwith two-frequency excitation. *Meccanica* **38**, 711–717. (doi:10.1023/A:1025817022623)

Canudas de Wit, C., Olsson, H., Åström, K. J. & Lischinsky, P. 1995 A new model for control of systems with friction. *IEEE Trans. Automat. Contr.* **40**, 419–425. (doi:10.1109/9.376053)

Coulomb C. A. 1785 *Théorie des machines simples*, vol. 10. Mémoires de Mathématique et de Physique de l'Academie des Sciences, pp. 161–331.

Courtney-Pratt, J. S. & Eisner, E. 1956 The effect of a tangential force on the contact of metallic bodies. *Proc. R. Soc. A* **238**, 529–550. (doi:10.1098/rspa.1957.0016)

Dahl, P. 1968 A solid friction model. Technical report TOR-0158(3107-18)-1, The Aerospace Corporation, El Segundo, CA.

Den Hartog, J. P. 1931 Forced vibrations with combined Coulomb and viscous friction. *Trans. ASME* **53**, 107–115.

Fenny, B. F. & Moon, F. C. 1994 Chaos in a forced dry friction oscillator: experiment and numerical modelling. *J. Sound Vib.* **170**, 303–323. (doi:10.1006/jsvi.1994.1065)

Haessig, D. A. & Friedland, B. 1991 On the modelling and simulation of friction. *J. Dyn. Syst. Measure. Contr. Trans. ASME* **113**, 354–362.

Harnoy, A. & Friedland, B. 1994 Modeling and simulation of elastic and friction forces in lubricated bearings for precise motion control. *Wear* **172**, 155–165. (doi:10.1016/0043-1648(94)90283-6)

Hess, D. P. & Soom, A. 1990 Friction at a lubricated line contact operating at oscillating sliding velocities. *J. Tribol.* **112**, 147–152.

Hinrichs, N., Oestreich, M. & Popp, K. 1998 On the modelling of friction oscillators. *J. Sound Vib.* **216**, 435–459. (doi:10.1006/jsvi.1998.1736)

Hunt, J. B., Torbe, I. & Spencer, G. C. 1965 The phase–plane analysis of sliding motion. *Wear* **8**, 455–465. (doi:10.1016/0043-1648(65)90138-9)

Johannes, V. I., Green, M. A. & Brockley, C. A. 1973 The role of the rate of application of the tangential force in determining the static friction coefficient. *Wear* **24**, 381–385. (doi:10.1016/0043-1648(73)90166-X)

Lampaert, V., Al-Bender, F. & Swevers, J. 2004 Experimental characterization of dry friction at low velocities on a developed tribometer setup for macroscopic measurements. *Tribol. Lett.* **16**, 95–105. (doi:10.1023/B:TRIL.0000009719.53083.9e)

Liang, J.-W. & Feeny, B. F. 1998*a* Dynamical friction behavior in a forced oscillator with a compliant contact. *J. Appl. Mech.* **65**, 250–257.

Liang, J.-W. & Feeny, B. F. 1998*b* Identifying Coulomb and viscous friction from free-vibration decrements. *Nonlin. Dynam.* **16**, 337–347. (doi:10.1023/A:1008213814102)

Liang, J.-W. & Feeny, B. F. 1998*c* A comparison between direct and indirect friction measurements in a forced oscillator. *J. Appl. Mech.* **65**, 783–786.

McMillan, A. J. 1997 A non-linear friction model for self-excited vibrations. *J. Sound Vib.* **205**, 323–335. (doi:10.1006/jsvi.1997.1053)

Oestreich, M. 1998 *Untersuchung von Schwingern mit nichtglatten Kennlinien*, Fortschr.-Ber. VDI Reihe 11 Nr. 258. Dusseldorf, Germany: VDI Verlag. [In German.]

Olsson, H., Åström, K. J., Canudas de Wit, C., Gäfvert, M. & Lischinsky, P. 1998 Friction models and friction compensation. *Eur. J. Control* **4**, 176–195.

Popp, K. & Stelter, P. 1990 Non-linear oscillations of structures induced by dry friction. In *Non-linear dynamics in engineering systems* (ed. W. Schiehlen). New York, NY: Springer.

Powell, J. & Wiercigroch, M. 1992 Influence of non-reversible Coulomb characteristics on the response of a harmonically excited linear oscillator. *Mach. Vib.* **1**, 94–104.

Rabinowicz, E. 1951 The nature of the static and kinetic coefficients of friction. *J. Appl. Phys.* **22**, 1373–1379. (doi:10.1063/1.1699869)

Ramberg W. & Osgood W. R. 1943 Description of stress–strain curves by three parameters. Technical note 902. Washington, DC: National Advisory Committee for Aeronautics.

Shaw, S. W. 1986 On the dynamic response of a system with dry friction. *J. Sound Vib.* **108**, 305–325. (doi:10.1016/S0022-460X(86)80058-X)

Shinozuka, M. & Deodatis, G. 1992 Simulation of stochastic processes by spectral representation. *Appl. Mech. Rev.* **44**, 191–203.

Shinozuka, M. & Jan, C.-M. 1972 Digital simulation of random processes and its applications. *J. Sound Vib.* **251**, 111–128. (doi:10.1016/0022-460X(72)90600-1)

Stefański, A., Wojewoda, J. & Furmanik, K. 2001 Experimental and numerical analysis of self-excited friction oscillator. *Chaos Soliton. Fract.* **12**, 1691–1704. (doi:10.1016/S0960-0779(00)00136-3)

Stefański, A., Wojewoda, J., Wiercigroch, M. & Kapitaniak, T. 2003 Chaos caused by non-reversible dry friction. *Chaos Soliton. Fract.* **16**, 661–664. (doi:10.1016/S0960-0779(02)00451-4)

Stribeck R. 1902 Die wesentlichen Eigenschaften der Gleitund Rollenlager—the key qualities of sliding and roller bearings. In *Zeitschrift des Vereines Deutscher Ingenieure*, no. 46(38,39), pp. 1342–1348, 1432–1437.

Tolstoi, D. M. 1967 Significance of the normal degree of freedom and natural normal vibrations in contact friction. *Wear* **10**, 199–213. (doi:10.1016/0043-1648(67)90004-X)

Tustin, A. 1947 The effects of backlash and of speed-dependent friction on the stability of closed-cycle control systems. *J. Inst. Electr. Eng.* **94**, 143–151.

Wiercigroch, M. 1993 Comments on the study of a harmonically excited linear oscillator with a Coulomb damper. *J. Sound Vib.* **167**, 560–563. (doi:10.1006/jsvi.1993.1354)

Wiercigroch, M. 1994 A note on the switch function for the stick-slip phenomenon. *J. Sound Vib.* **175**, 700–704. (doi:10.1006/jsvi.1994.1559)

Wiercigroch, M. & Cheng, A. D.-H. 1997 Chaotic and stochastic dynamics of orthogonal metal cutting. *Chaos Soliton. Fract.* **8**, 715–726. (doi:10.1016/S0960-0779(96)00111-7)

Wiercigroch, M., Sin, V. W. T. & Liew, Z. F. K. 1999 Non-reversible dry friction oscillator: design and measurements. *Proc. Inst. Mech. Eng.* **213**, 527–534.

Wojewoda, J. 1992 Chaotic behavior of friction force. *Int. J. Bifurcat. Chaos* **2**, 205–209.

Wojewoda, J., Kapitaniak, T., Barron, R. & Brindley, J. 1993 Complex behaviour of a quasiperiodically forced system with dry friction. *Chaos Soliton. Fract.* **3**, 35–46. (doi:10.1016/0960-0779(93)90038-3)